Preparation and Characterization of Monodisperse FePd Nanoparticles

Yanglong Hou,† Hiroshi Kondoh,† Toshihiro Kogure,‡ and Toshiaki Ohta*,†

Department of Chemistry and Department of Earth and Planetary Science, School of Science, The University of Tokyo, Tokyo 113-0033, Japan

Received July 7, 2004. Revised Manuscript Received September 9, 2004

Monodisperse FePd nanoparticles were prepared by polyol reduction of palladium acetylacetonate and thermal decomposition of iron pentacarbonyl, using a combination of *n*-adamantanecarboxylic acid and tri-alkylphosphine as stabilizers. The mean particle size can be tuned from 11 to 16 nm by controlling the concentration and type of stabilizers and reaction conditions. High monodispersity of FePd nanoparticles leads to the formation of two-dimensional (2D) superlattices consisting of hexagonal close-packed particles, which was confirmed by X-ray diffraction pattern and high-resolution transmission electron microscopic (HRTEM) images. This route provides a promising candidate for studying the magnetic properties of nanosized FePd materials.

Introduction

Magnetic nanoscale materials have attracted much attention owing to their potential applications in magnetic recording devices, medical diagnoses and magnetooptical systems.[1−4] As well known, the physical and chemical properties of nanoscale materials are highly dependent on the size, morphology, crystal defects, and monodispersity of nanocrystals.[5−8] Preparation of high-quality magnetic nanoscale materials is indispensable for their further applications.[9,10] In recent developments, the preparation of monodisperse magnetic nanocrystals has been successfully achieved by a high-temperature organometallic route. For example, monodisperse FePt nanocrystals were prepared by hydrolysis of pentacarbonyl iron and reduction of metal complexes in the presence of oleic acid and oleylamine.[2] Such an approach was extended to prepare $Fe_xCo_yPt_z$,[11] $CoPt_3$,[12] Fe,[13] Fe_2O_3,[14] and ferrite[15] nanocrystals. Among these magnetic materials, FePt, CoPt, and FePd alloys with high magnetocrystallic anisotropy and chemical stability inspired much interest because of their potential applications in high-density data storage and high-performance permanent magnets. Because the magnetic stability of an individual particle is related to the anisotropy constant and the particle volume, these alloys become promising candidates to fabricate ultra-high-density magnetic storage devices. Normally, FePd thin films have been mainly prepared by vacuum deposition technology.[4] Until now, a number of efforts have been devoted to prepare monodisperse magnetic or semiconductor nanocrystals via a wet chemical method with binary or multiple surfactants, such as trioctylphosphine oxide (TOPO)-oleic acid,[3] adamantanelcarboxylic acid (ACA)-hexadylamine (HDA),[13] HDA-TOPO-TOP.[16] However, the formation of monodisperse FePd nanocrystals has been barely successful. Very recently, Harrell's group has succeeded in preparing

* To whom correspondence should be addressed. Fax: 81-3-38121896. Tel: 81-3-58414333. E-mail: ohta@chem.s.u-tokyo.ac.jp.
† Department of Chemistry.
‡ Department of Earth and Planetary Science.

(1) (a) Murray, C. B.; Sun, S.; Doyle, H.; Betley, T. *Mater. Res. Soc. Bull*. **2001**, 985. (b) Leslie-Pelecky D. L.; Rieke, R. D. *Chem. Mater*. **1996**, *8*, 1770. (c) Hyeon, T. *Chem. Commun*. **2003**, 927.
(2) Sun, S.; Murray, C. B.; Weller, D.; Folks, L.; Moser, A. *Science* **2000**, *287*, 1989.
(3) Puntes, V. F.; Krishnan, K. M.; Alivisatos, A. P. *Science* **2001**, *291*, 2115.
(4) (a) Weller, D.; Doerner, M. F. *Annu. Rev. Mater. Sci*. **2000**, *30*, 611. (b) Medina R.; Parra, R. E. *J. Appl. Phys*. **1982**, *53*, 2201. (c) Armelles, G.; Weller, D.; Rellinghaus, B.; Farrow, R. F. C.; Toney, M. F. *IEEE Trans. Magn*. **1997**, *33*, 3220.
(5) (a) Hu, J.; Odom, T. W.; Lieber, C. M. *Acc. Chem. Res*. **1999**, *32*, 435. (b) Xia, Y.; Yang, P.; Sun, Y.; Wu, Y.; Mayers, B.; Gates, B.; Yin, Y.; Kim, F.; Yan, H. *Adv. Mater*. **2003**, *15*, 353. (c) Nath, M.; Choudhury, A.; Kundu, A.; Rao, C. N. R. *Adv. Mater*. **2004**, *15*, 2098. (d) Li, W.; Wang, X.; Li, Y. *Chem. Commun*. **2004**, 164.
(6) (a) Feldheim, D. L.; Foss, C. A., Jr., Eds. *Metal Nanoparticles: Synthesis, Characterization and Applications;* Dekker: New York, 2002. (b) Klabunde,K. J., Ed. *Nanoscale Materials in Chemistry*; John Wiley & Sons: New York, 2001.
(7) (a) Breulmann, M.; Colfen, H.; Hentze, H. P.; Antonietti, M.; Walsh, D.; Mann, S. *Adv. Mater*. **1998**, *10*, 237. (b) Teranishi, T.; Hasegawa, S.; Shimuzu, T.; Miyake, M. *Adv. Mater*. **2001**, *13*. 1699.
(8) (a) Sun, S.; Murray, C. B. *J. Appl. Phys*. **1999**, *85*, 4325. (b) Legrand, J.; Ngo, A. T.; Petit, C.; Pileni, M. P. *Adv. Mater*. **2001**, *13*, 58. (c) Hou Y.; Gao, S. *J. Mater. Chem*. **2003**, *13*, 1510.
(9) (a) Dumestre, F.; Chaudret, B.; Amiens, C.; Renaud, P.; Fejes, P. *Science* **2004**, *303*, 821. (b) Green, M.; O'Brien, P. *Chem. Commun.* **2001**, 1912.
(10) (a) Zhang, X. X.; Wei, H. L.; Zhang, Z. Q.; Zhang, L. *Phys. Rev. Lett*. **2001**, *87*, 157203. (b) Cheon, J.; Kang, N. J. Lee, S. M.; Lee, J. H.; Yoon, J. H.; Oh, S. J. *J. Am. Chem. Soc*. **2004**, *126*, 1950. (c) Hou, Y.; Yu, J.; Gao, S. *J. Mater. Chem*. **2003**, *13*, 1983. (d) Hou, Y.; Gao, S.; Ohta, T.; Kondoh, H. *Eur. J. Inorg. Chem.* **2004**, 1169.
(11) Chen, M.; Nikles, D. E. *Nano Lett.* **2002**, *2*, 211.
(12) (a) Shevchenko, E. V.; Talapin, D. V.; Schnablegger, H.; Kornowski, A.; Festin, Ö.; Svedlindh, P.; Haase, M.; Weller, H. *J. Am. Chem. Soc*. **2003**, *125*, 9090. (b) Shevchenko, E. V.; Talapin, D. V.; Rogach, A. L.; Haase, M.; Weller, H. *J. Am. Chem. Soc*. **2001**, *124*, 11480. (c) Wiekhorst, F.; Shevchenko, E.; Weller, H.; Kötzler, J. *Phys. Rev.* **2003**, *B67*, 224416.
(13) Suslick, K. S.; Fang, M.; Heyon, T. *J. Am. Chem. Soc*. **1996**, *118*, 11960.
(14) Hyeon, T.; Lee, S. S.; Park, J.; Chung, Y.; Na, H. B. *J. Am. Chem. Soc.* **2001**, *123*, 12798.
(15) (a) Sun, S.; Zeng, H.; Robinson, D. B.; Raoux, S.; Rice, P. M.; Wang, S. X.; Li, G.; *J. Am. Chem. Soc*. **2004**, *126*, 273. (b) Sun S.; Zeng, H. *J. Am. Chem. Soc*. **2002**, *124*, 8204.
(16) Talaphin, D. V.; Rogach, A. L.; Kormowski, A.; Haase, M.; Weller, H. *Nano Lett*. **2002**, *1*, 207.

10.1021/cm048902c CCC: $27.50
Published on Web 11/03/2004

FePd and FePdPt nanoparticles. But as they stated, further works are needed to narrow the size distribution for the particles larger than 9 nm.[17]

Experimental Section

To prepare highly monodisperse FePd nanoparticles, we used a combination of ACA and alkylphosphine to stabilize FePd nanocrystals. The chemical synthetic route is a modification of the approach used by Sun et al.[2] that is based on the reduction of $Pd(acac)_2$ (acac = acetylacetonate) with hexadecanediol and thermal decomposition of $Fe(CO)_5$. Note that the combination of ACA and tributylphosphone (TBP) or oleic acid plays a key role for preparing monodisperse FePd nanoparticles. The 2D assembled nanostructures of FePd were also obtained, suggesting high monodispersity of FePd nanoparticles. The size and composition of FePd nanoparticles can be readily controlled by adjusting the combination of various stabilizers and the reaction condition. For example, with 4:1 molar ratio of $Fe(CO)_5$ to $Pd(acac)_2$, $Fe_{28}Pd_{72}$ particles (sample a) were produced by using oleic acid-TBP as stabilizers, while $Fe_{50}Pd_{50}$ particles (sample b) were produced by using ACA-TBP as the stabilizers (see Supporting Information). The chemical composition of each sample was determined by using a Fisons Kevex energy disperse X-ray detector in a transmission electron microscope (TEM, Hitachi HF-2000).

The reaction process was followed by the standard Schlenk-line technique. In a typical synthesis, under Ar atmosphere protection conditions, 0.08 g of $Pd(acac)_2$ (0.25 mmol), and 0.54 g (3 mmol) of ACA were dissolved in 1 mL of TBP to form Pd-TBP-ACA mixture at room temperature. Subsequently, 0.14 mL of $Fe(CO)_5$ (1 mmol) was injected into the mixture of Pd-TBP-ACA. After stirring for 30 min, orange stock solution of the Fe−Pd-TBP-ACA complex was obtained. In a separate flask, the reducing solution consisting of 390 mg of hexadecanediol and 15 g of TBPO was heated to 120−180 °C and bubbled with Ar for 60 min. Sequentially, the Fe−Pd-TBP-ACA stock solution was quickly injected into the reducing solution, and the reaction temperature was slowly increased and maintained at 280−300 °C for 30−60 min. The color slowly changed from orange to black, indicating the formation of FePd nuclei. After the designated time, the heater was removed and the solution was cooled to room-temperature naturally. The post-prepared process was performed in air. The black precipitates were isolated from the solution by adding nonpolar solvent such as ethanol or acetone and centrifuging. If necessary, a cycle of the washing process with hexane and acetone was performed.

Results and Discussion

The morphologies and the crystal lattice structures of FePd nanoparticles were observed with the TEM (Hitachi HF-2000) with an accelerated voltage of 200 kV. The TEM image (Figure 1a) shows that FePd nanoparticles with the diameter of 11 nm are well arranged in a 2D nearly hexagonal close-packed array, demonstrating the monodisperse particle size distribution (see Supporting Information). These particles were obtained without any further post-preparative process, the so-called size-selective approach.[18] The high resolution TEM (HRTEM) image in Figure 1b indicates that FePd particles have a well-defined crystallinity. Fast Fourier transform (FFT) pattern (Figure 1c) also confirms a highly crystalline nature. The electron diffraction (ED) pattern (Figure 1d) exhibits three diffused

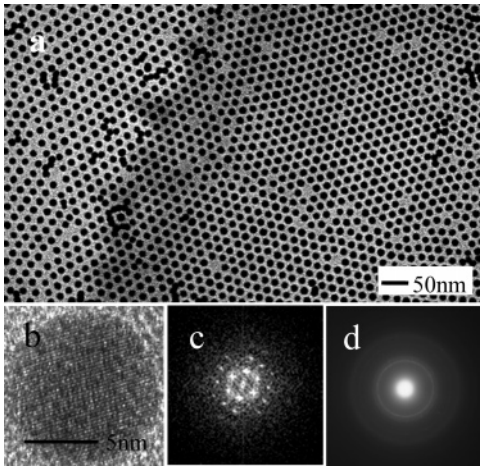

Figure 1. TEM image (a), high-resolution TEM image (b), fast Fourier transform (FFT) (c), and electron diffraction (ED) pattern (d) of 11-nm $Fe_{28}Pd_{72}$ nanoparticles.

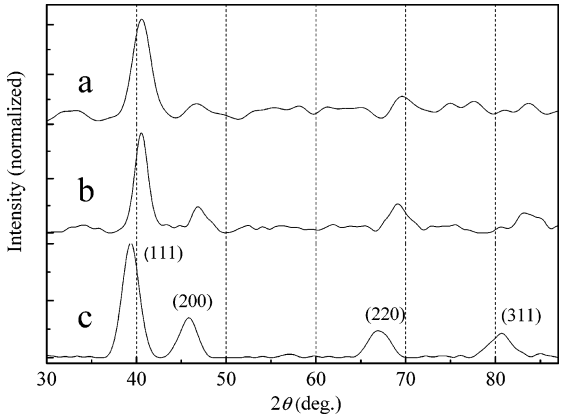

Figure 2. XRD patterns of the samples compared with that of Pd nanoparticles: (a) sample a, (b) sample b, and (c) Pd nanoparticles.

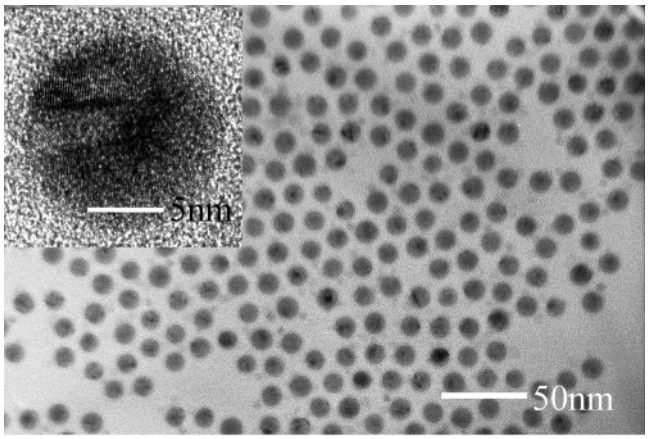

Figure 3. TEM image of 16-nm $Fe_{50}Pd_{50}$ particles. The inset is a high-resolution TEM image of a single particle.

rings, which should be assigned to (111), (220), and (311) reflections of cubic FePd. The X-ray diffraction pattern (XRD) of FePd nanoparticles confirms that as-synthesized FePd particles belong to a chemically disordered cubic structure (Figure 2a). The position of (111) peak in FePd has an obvious shift to the higher angle, compared to Pd nanoparticles, which further confirms the formation of FePd alloys.[19]

To obtain large FePd nanoparticles, a combination of ACA and TBP was employed. As shown in Figure 3,

(17) (a) Chen, M.; Nikles, D. E. *J. Appl. Phys*. **2002**, *91*, 8477. (b) Kang, S.; Jia, Z.; Nikles, D. E.; Harrell, J. W. *J. Appl. Phys*. **2004**, *95*, 6744.

(18) (a) Weller, H. *Angew. Chem., Int. Ed*. **1993**, *32*, 41. (b) Reetz, M. T.; Maase, M. *Adv. Mater*. **1999**, *11*, 9.

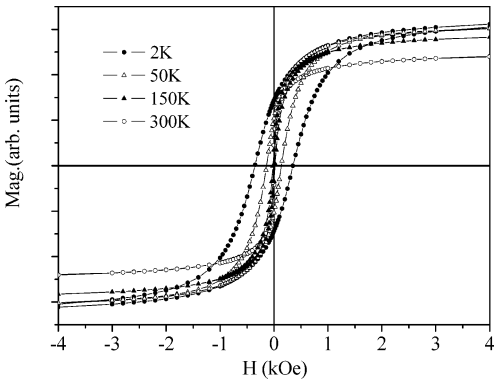

Figure 4. Hysteresis loops of 16-nm $Fe_{50}Pd_{50}$ nanoparticles at 2, 50, 150, and 300 K.

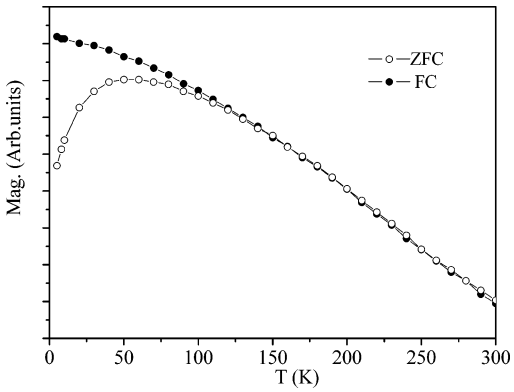

Figure 5. ZFC−FC curves of 16-nm $Fe_{50}Pd_{50}$ nanoparticles measured at a magnetic field of 100 Oe.

FePd (sample b) has also a nearly monodisperse structure. The inset shows a well-defined crystallinity. The XRD pattern of sample b is displayed in Figure 2b. The particle size was calculated to be 16 nm by Scherrer's formula, which is in good agreement with the value observed by TEM. Broadening of the (111) peak from sample b to a matches with the change of the sample size. Although the XRD patterns (see Figure 2) accord with that of the bulk FePd, the formation of segregated nanophase or core−shell phase cannot be ruled out completely from these data. We believe, however, that these processes do not occur under the present condition by the following reasons: (1) Iron can be easily recognized in TEM in the background of Pd and FePd because of extremely high contrast.[19] The observed TEM image, however, did not show any evidence of isolated Fe shells or clusters. (2) The higher symmetry of the hysteresis loops mostly rules out the presence of FePd poly-phase in the sample (see the magnetic properties below). Due to their narrow size distribution, FePd nanoparticles have a strong tendency to self-assemble into hexagonal 1D and 2D superlattice structures. The assembly of FePd nanoparticles forms different geometric patterns depending on the particle size and evaporation condition of the solvent with FePd nanoparticles.

Although the formation mechanism of FePd nanoparticles has not yet been fully understood, it is generally accepted that the process begins with rapid nucleation and growth of nuclei into smaller clusters. TBP and ACA were used as capping agents to tune the growth of nanoclusters. Linear-shaped TBP forms a tight micelle structure and limits the growth of metal nuclei.[20] In contrast with TBP, bulky ACA with adamantly end groups would not have strong coordination to the metal clusters, leading to high surface free energy. This is why the particles grow to larger sizes and crystallize easily, which is different from the case of fatty acids.[11,13] The capping agents allow the particles to be dissolved in nonpolar solvents and prevent them from agglomeration and oxidation.

Magnetic measurement on FePd (16 nm) nanoparticles indicates that the particles are superparamagnetic at room temperature, meaning that the thermal energy can overcome the anisotropy energy barrier of a single particle and the net magnetization of the particle assembly is zero in the absence of an external field. Figure 4 shows the hysteresis loop of 16 nm FePd nanoparticles at different temperatures. One can see that the particles are ferromagnetic with the coercivity of 350 Oe at 2 K and 140 Oe at 50 K, whereas the coercivity is negligible at room temperature. Sato and Hirotsu observed a weak shoulder in the hysteresis loop of FePd nanoparticles prepared by the electron beam evaporation technique. This shoulder indicates a presence of $L1_0$−FePd nanoparitcles with different anisotropy constant K_u. The variety of K_u must be due to the distribution of the alloy composition with the particles.[21] The hysteresis loop of our sample has a highly symmetric shape, mostly suggesting the absence of polyphases of FePd in the sample. For smaller FePd nanoparticles, saturation magnetization decreases, which might result from surface spin canting of the nanoparticles.[15] Zero-field-cooling (ZFC) and field-cooling (FC) curves indicate that the blocking temperature of 16-nm $Fe_{50}Pd_{50}$ nanoparticles is 50 K, as shown in Figure 5. From the ZFC−FC data, K_u of the 16-nm as-synthesized FePd nanoparticles was estimated to be 1.6×10^4 J/m^3 by using the equation, $K_u = \langle 48k_BT \rangle / \langle V \rangle$, where k_B is the Boltzmann constant, T is the temperature, and V is the volume.[2] The value obtained is much smaller than that of bulk materials (2.6×10^6 J/m^3).[22] It is mostly attributed to chemical disorder state of as-synthesized FePd nanoparticles.

Conclusion

In conclusion, combinations of TBP and ACA or oleic acid have been applied to prepare monodisperse size-controlled FePd nanoparticles. The size control of nanoparticles between 11 and 16 nm can be achieved by tuning the equilibrium between the nucleation and growth rates. Further studies show that the process is not limited to FePd nanoparticles but can be extended to other types of monodisperse metal nanoparticles.

Acknowledgment. This work was supported in part by the Japan Society of the Promotion of Science (JSPS)

(19) (a) Wunder, R.; Philips, J. *J. Phys. Chem*. **1996**, *100*, 14430. (b) Wunder, R.; Philips, J. *J. Phys. Chem.* **1994**, *98*, 12329. (c) Pérez-Landazábal, J. I.; Gómez-Polo, C.; Recart, V.; Vergara, J.; Ortega, R. J. *J. Magn. Magn. Mater*. **1999**, *196−197*, 179. (c) Teranishi, T.; Miyaki, M. *Chem. Mater*. **1999**, *11*, 3414.

(20) Peng, X.; Wickham, J.; Alivisatos, A. P. *J. Am. Chem. Soc*. **1998**, *120*, 5343.

(21) Sato, K.; Hirotsu, Y. *J. Appl. Phys*. **2003**, *93*, 6291. (b) Matsui, M.; Adachi, K. *Phys. B* **1989**, *161*, 53. (c) Sato, K.; Bian, B.; Hirotsu, Y. *J. Appl. Phys*. **2002**, *91*, 8516.

(22) Kussmann, A.; Müller, K. *Angew. Phys*. **1964**, *17*, 509.

and the 21st Century COE Program from the Ministry of Education, Culture, Sports, Science and Technology.

Supporting Information Available: Energy dispersive patterns and particle size distributions of samples. This material is available free of charge via the Internet at http://pubs.acs.org.

CM048902C